Infrared Thermography to Study Damage During Static and Cyclic Loading of Composites

Rosa De Finis[✉], Davide Palumbo, and Umberto Galietti

Politecnico di Bari, Via Orabona, 5, 70125 Bari, Italy
`rosa.definis@poliba.it`

Abstract. The anisotropy and heterogeneity of composites influence unavoidably the mechanical response of the material to external excitation and the failure mechanisms. As an effect, the mechanical behaviour assessment of composites by means of experimental techniques requires to pay attention to the influence of the specific layup of laminae, viscous properties of the matrix, pattern described by the yarns or fibers. It follows that specific quantitative and qualitative analysis are required for the data processing.

The study of thermal signal can be a successful strategy to assess and to understand the damage processes. In effect, if compared to other experimental techniques, it allows a localised analysis of the material degradation in terms of stiffness reduction or damage progression (transverse cracks or delamination).

The present research is aimed at providing innovative methods and algorithms for processing the thermal signal of a composite obtained by Automated Fiber Placement process, in order to determine when and where damage occurred during static and cyclic loading in terms of transverse crack number.

Keywords: CFRP · Automated fiber placement · Thermal signal analysis · Damage · Crack number

1 Introduction

The damage mechanisms in composites are a crucial aspect of the structural health monitoring and the fatigue life assessment [1–5].

The analysis of the thermal signal [2] can be a valid tool to support the understanding and assessment of damage in composites. By carrying out a suitable processing procedures of the data it is possible to quantitatively estimate the damage in composites [6]. The adopted parameters for the analysis are specifically the components extracted by the measured thermal signal: the component related to the mean temperature increase, the thermoelastic component [4] and the one associated with energy dissipations [5].

Damage in composites is characterized by the occurrence of specific damage stages of different mechanisms [7–9]. The transverse cracks are typical of a first damage stage while delamination and fiber breakage are specific of the second and the third stages. Specific damage state occurs during the delamination regime, where the damage achieves a fixed value called Characteristic Damage State (CDS) [10–12]. The CDS is important

to understand the material damage progression. A similar damage behaviour is present under the application of static load [13, 14].

To evaluate the structural health of the material an appropriate damage parameter can be the number of transverse cracks appearing under cyclic and static loadings [13–18], that is also related to the material mechanical properties degradation [19, 20].

The adopted techniques to measure the cracks number are the optical microscopy [16] and acoustic emission techniques [21]. The major difficulties in the experimental evaluation of the crack number are related to the identification of the cracks and in the evaluation of the crack length [18] coupled with a complex setup and suitable material preparation.

In the present work, the thermal signal analysis is showed capable of estimating the damage in terms of crack number of a quasi-isotropic CFRP composite obtained by Automated Fiber Placement under both static and cyclic (two different stress levels) loading. In particular, the temperature signal was acquired during the loading tests and specific data processing procedures of thermal signal components are proposed for measuring number of cracks. The crack number evaluation leads to evaluate the Characteristic Damage State under both static and cyclic load.

2   Experimental Campaign

Automatic Fiber Placement technology is an innovative technology aimed at deposing composite layers as unidirectional prepreg tapes [3]. The tested material is a quasi-isotropic CFRP with a layup of [0/-45/45/90/90/45/-45/0]$_2$. Sample dimensions are 25 mm width, 250 mm length and 3.0 mm thick. All the specimens are tested on servo-hydraulic loading frame INSTRON 8850 (250 kN capacity) that was equipped also with a clip on extensometer (gage length 25 mm) providing strain measurements.

Three samples were addressed to static tensile tests at 1 mm/min of displacement rate according to the Standard [22]. The obtained ultimate tensile strength (UTS) of material is 825 MPa (standard deviation 84.57 MPa). The tests were monitored by IR camera FLIR X6540 SC that acquired at a frequency of 15 Hz.

The fatigue tests were carried out on two samples undergoing constant amplitude stresses (runout 2 * 10ˆ6 cycles) at a stress ratio of 0.1 and a loading frequency of 7 Hz. The cyclic tests were monitored by using the same infrared detector as the one used for tensile tests, the acquisition frequency was set to 177 Hz. The acquired sequences were of 1770 frames. Each thermal acquisition corresponded to specific loading cycles. For the measurements of the crack number, two samples have been considered: the sample tested at 50% UTS and the one tested at 80% UTS, the applied loading stress is expressed in terms of ultimate tensile strength.

Fig. 1 describes the setup and layout of the adopted equipment.

3   Data Processing

The thermal signal data from tensile and cyclic tests have been processed by using two different data processing procedures as the temperature variations are clearly different during a static and a cyclic tests.
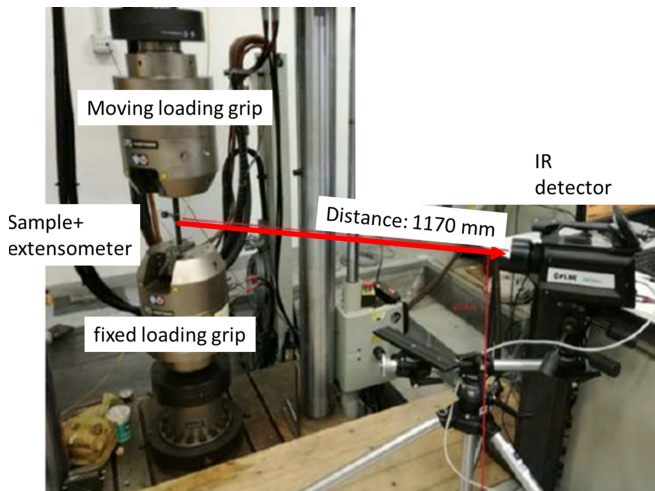
Fig. 1. Equipment and layout

3.1 Temperature Data from Static Tests

The measured data from the infrared detector require a specific processing procedure as they are affected by thermal gradients through the sample, material fabric pattern etc.…

In Fig. 2, the thermal signals from tensile tests are reported. The signal refers to the area in the gage length of the sample. The curves of Fig. 2 present the characteristic decreasing phase related to the thermoelastic effect [4, 6]. The noisy behaviour of the signal is due to the incoming cracks in the matrix. This leads to some issues in evaluating the cracks occurring in the matrix as the total gradient through the sample is basically higher than the temperature variation associated to a crack. So that, a specific procedure is essential for detecting and measuring the number of transverse cracks. In this way, the data are analyzed by a suitable Matlab® routine operating on temperature tridimensional matrixes where each pixel value represents a temperature value at specific time instant. The processing procedure involves the following steps:

- Subtraction from each matrix at a specific time instant the data matrix from previous time instant (dynamic frame subtraction);
- Re-sizing of the temperature maps through the frames in order to eliminate the backstage from image;
- Assessing the 98° percentile from each data matrix (threshold for the following step);
- Matrix binarization by comparing the value of each pixel with the extracted percentile;
- Counting for each row (minimum 15 pixels) the pixel values above the threshold;
- Assessing the instantaneous crack number and cumulated crack number. This latter is normalized by the inspected length (roughly 150 mm for each sample).

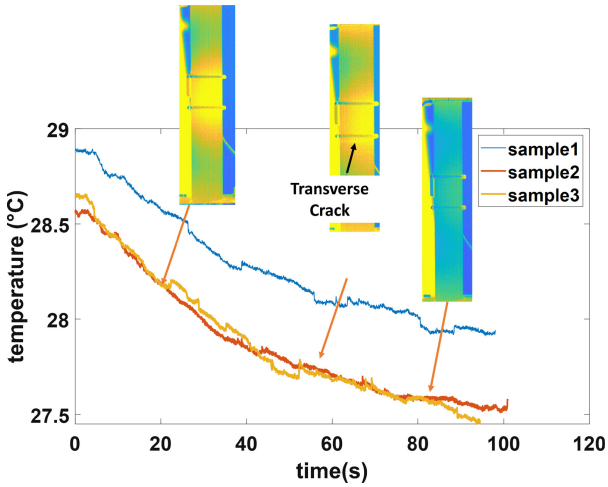The stages of the procedure are represented by the maps in Fig. 3.

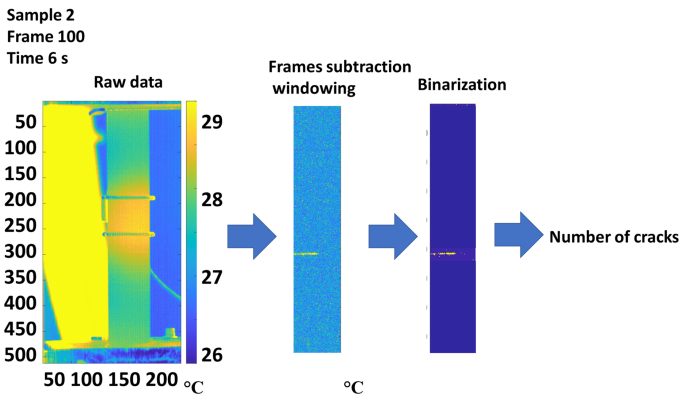**Fig. 2.** Temperature profiles for samples 1, 2, 3.

Fig. 3. Maps of the steps of proposed procedure on sample 2 at initial time instants of the test.

3.2 Temperature Data Acquired During Cyclic Tests

The thermal sequences of a sample tested at 50% UTS and a sample tested at 80% UTS acquired during cyclic tests were processed by using a specific algorithm providing the thermal signal reconstruction by means of the least square method [5, 6]. In the case of cyclic load the damage mechanisms are complicated by the fact that typical damage phenomena can occur separately or concurrently, so that they can interact each other [13, 19] resulting in a complex thermal response. In this case, it is better to refer for crack number assessment to a more local parameter.

The following model presents a separation of the different temperature components of the thermal signal:

$$S(t) = S_m + S_{1\omega}(\sin(\omega t + \varphi_1)) + S_{2\omega}(\sin(2\omega t + \varphi_2)) + S_{3\omega}(\sin(3\omega t + \varphi_3))$$
$$+ .. + S_{n\omega}(\sin(n\omega t + \varphi_n)) \tag{1}$$

S_m is the mean temperature signal, $S_{1\omega}, S_{2\omega}, S_{3\omega},...S_{n\omega}$ represent respectively the amplitude harmonic components at one-twice-triple-..-umpteenth times the mechanical frequency while $\varphi_1, \varphi_2, \varphi_3$ φ_n are respectively the phase shifts. The adopted thermal metric for detecting and measuring the transverse crack is $S_{2\omega}$.
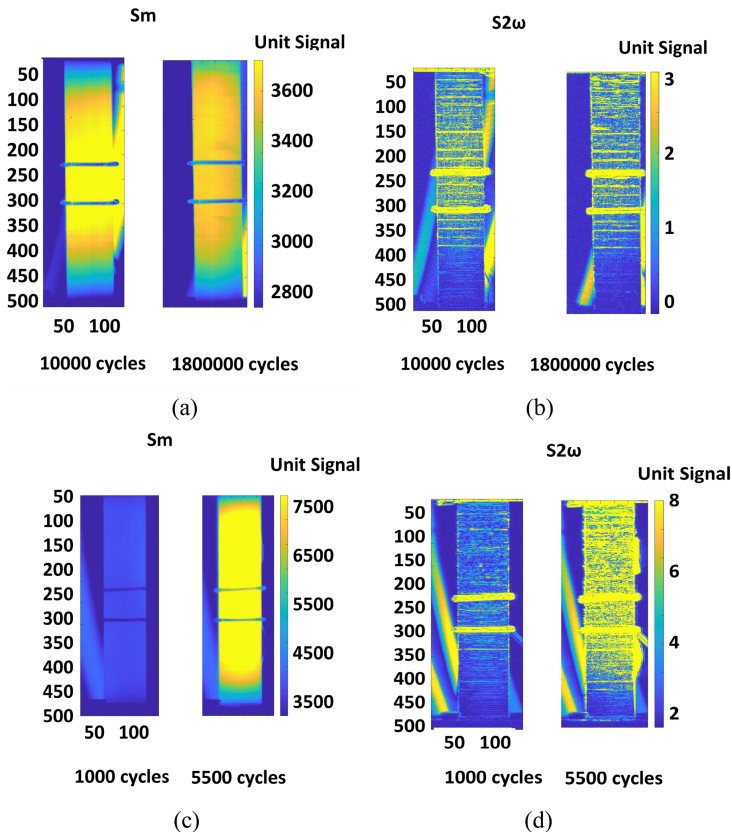

Fig. 4. Maps of S_m and $S_{2\omega}$ for samples tested at: (a−b) 50% UTS and (c−d) 80% UTS.

In Fig. 4 the maps of S_m for the stress levels 50% UTS (Fig. 4a) and 80% UTS (Fig. 4c) are compared to the related $S_{2\omega}$ maps (Fig. 4b−d). The effect of the stress increased from 50% UTS to 80% UTS, and is observable both in S_m and $S_{2\omega}$ maps. By comparing the figures it is also possible to understand the difference between the two metrics that are related to two different physics. In particular from $S_{2\omega}$ maps is easier to detect the transverse cracks than by using S_m.

The procedure to detect the transverse cracks from $S_{2\omega}$ signal maps is composed by the following steps:

- Applying a spatial dimension gaussian filter to reduce the noise;
- Reducing the $S_{2\omega}$ maps through the cycles in order to eliminate the backstage from image;
- Assessing the 98° percentile from each data matrix;
- Binarising the maps by comparing the value of each pixel with the extracted percentile;
- Counting for each row of the map the occurrences (minimum 15 pixels) of the values above the threshold;
- Assessing the cumulated crack number. This latter is normalized by the inspected length (roughly 150 mm for each sample).

In Fig. 5 the output in terms of binarized maps of $S_{2\omega}$ are presented. One firstly can observe that the effect of the stress on crack number is evident from lower imposed stress to the higher imposed stress. In particular, the more the imposed load is near the static tensile strength the more the signal is noisy and the assessment of the crack requires a specific smoothing procedure.
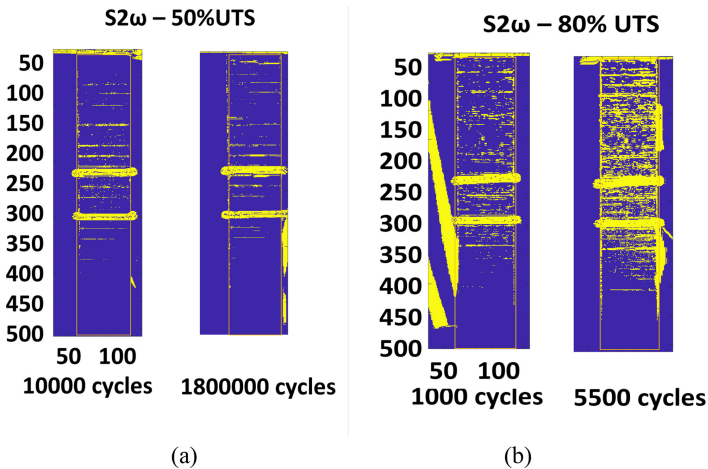

Fig. 5. Maps of $S_{2\omega}$ after binarization at two different number of cycles for: (a) the sample tested at 50% UTS and (b) the sample tested at 80% UTS.

4 Results and Discussion

In this section the results in terms of crack number are evaluated for samples addressed to tensile static and for cyclic tension-tension loads.

In Fig. 6 are represented the number of instantaneous (Fig. 6a) and cumulated cracks (Fig. 6b) assessed during the static tensile tests. The number of instantaneous cracks

appearing through the sample during the test is clearly discontinuous. It is also possible to observe that the appearance of cracks seems to start in a specific time instant for all the samples. This is more evident by observing the cumulated crack number normalized by sample length (crack density): the cracks start to increase after roughly 45−47s for samples 1 and 2, and after 60s for sample 3. The shift of the appearance of the cracks for sample 3 can be attributed to sample manufacturing i.e. presence of flaws. For samples 1 and 2 the stress at which the cracks start is 415 MPa (50% UTS) while for sample 3 the cracks start at 549 MPa (65% UTS).
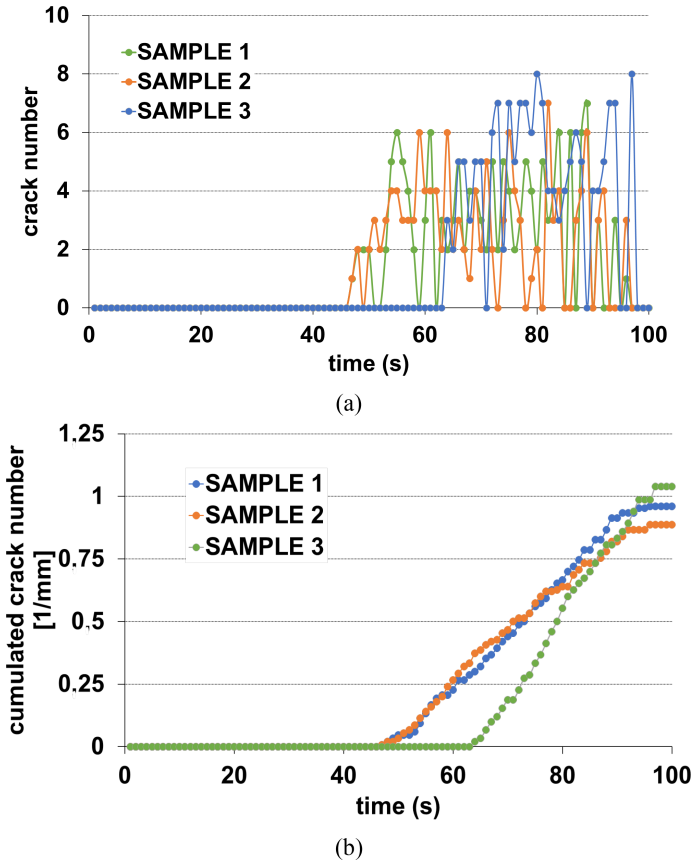

(a)

(b)

**Fig. 6.** Crack number during static tests: (a) instantaneous, (b) cumulated.

It is also interesting to observe that before the final failure there is the 'characteristic damage state' (CDS). In general, depending on the material, CDS for static tests is different from the one found during fatigue [13, 14].

The cumulated crack number is reported in Fig. 7 for fatigue tests performed at 50% and 80% UTS. In particular, Fig. 7a shows the results of crack density with respect the cycles number: for the sample tested at the lowest load it is possible to distinguish the

crack number saturation which is undistinguishable for the sample tested at 80% UTS. By considering the ratio cycles to total loading cycles (2,000,000 cycles) it is possible to observe the saturation in the crack densities Fig. 7b. Graphs of Fig. 7 show also the presence of the stress effect in the crack densities measurements.

The CDS obtained from fatigue tests start at about 0.2–0.3 cycles/total loading cycles according to the observation of literature [10–20].

The values of the crack densities measured during static and cyclic test are different in particular, those from static tension tests are higher than others. This could be explained by the different stages of damage involved in a static and cyclic test.
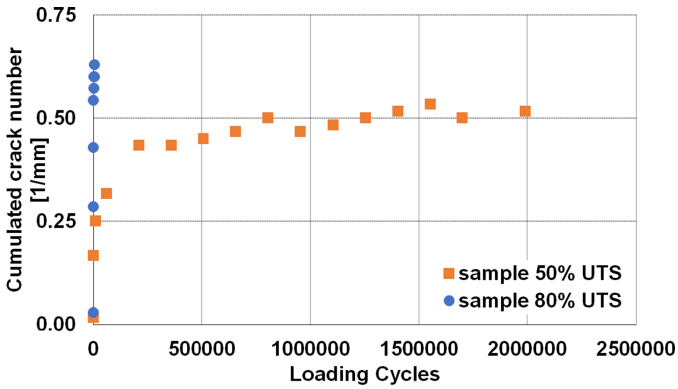
(a)
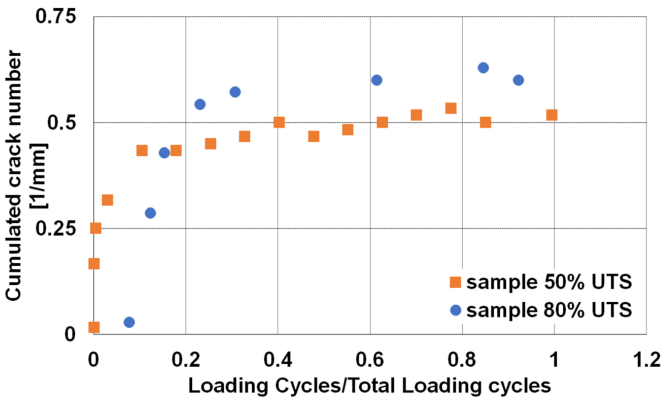
(b)

Fig. 7. (a) Cumulated crack number versus cycles, (b) cumulated crack number versus cycles/total cycles for two cyclic tests.

5 Conclusions

In this work, a quasi-isotropic CFRP made by automated fiber placement were tested both under static and cyclic loading. The tests were monitored by means of an infrared camera to measure the transverse crack number. In particular, three samples were tested under a static tensile load and two samples were tested at a cyclic load of 50% UTS and 80% UTS.

The comparison of the crack densities measured by using S_m and $S_{2\omega}$ show the appearance of cracks during static tests at stress ranging between 50–60% UTS and the presence of CDS achieved both during static and cyclic loads starting at 20–30% cycles/total cycles for fatigue tests. CDS is higher for the data of the static tests.

These results demonstrated the capability of the infrared thermography to measure the crack number and then the capability of studying damage during any kind of loading. This approach seems to be promising for those applications where it is difficult to measure the cracks. It can be also a tool for validating theoretical and numerical models.

References

1. Bannister, M.K.: Development and application of advanced textile composites. Proc. Inst. Mech. Eng. Part L J. Mater. Des. Appl. **218**, 253–260 (2004)
2. Palumbo, D., De Finis, R., Demelio, G.P., Galietti, U.: Early detection of damage mechanisms in composites during fatigue tests. In: Annual Conference and Exposition on Experimental and Applied Mechanics 2016. Conference Proceedings of the Society for Experimental Mechanics Series, vol. 8, pp. 133–141 (2016)
3. Schmidt, C., Denkena, B.: Thermal image-based monitoring for the automated fiber placement process. In: 10th CIRP Conference on Intelligent Computation in Manufacturing Engineering - CIRP ICME (2016)
4. Emery, T.R., Dulieu-Barton, J.K.: Thermoelastic stress analysis of the damage mechanisms in composite materials. Compos. Part A **41**, 1729–1742 (2010)
5. De Finis, R., Palumbo, D., Galietti, U.: A multianalysis thermography-based approach for the fatigue and damage investigation of ASTM A182 F6NM steel at two stress ratios. Fatigue Fract. Eng. Mater. Struct. **42**(1), 267–283 (2019)
6. De Finis, R., Palumbo, D., Galietti, U.: Evaluation of damage in composites by using thermoelastic stress analysis: a promising technique to assess the stiffness degradation. Fatigue Fract. Eng. Mater. Struct. (FFE) (2020). https://doi.org/10.1111/(ISSN)1460-2695
7. Heslehurst, R.B.: Defects and Damage in Composite Materials and Structures. CRC Press Taylor & Francis Group, Boca Raton (2014)
8. Huang, J., Pastor, M.J., Garnier, C., Gonga, X.J.: A new model for fatigue life prediction based on infrared thermography and degradation process for CFRP composite laminates. Int. J. Fatigue **120**, 87–95 (2019)

9. Degrieck, J., Van Paepegem, W.: Fatigue damage modeling of fibre-reinforced composite materials: review. Appl. Mech. Rev. **54**(4), 279–300 (2001)
10. Hashin, Z.: Analysis of composite materials. J. Appl. Mech. **50**, 481 (1983)
11. Stens, C., Middendorf, P.: Computationally efficient modelling of the fatigue behaviour of composite materials. Int. J. Fatigue **80**, 69–75 (2015)
12. Renard, J., Favre, J.P., Jeggy, T.H.: Influence of transverse cracking on ply behavior: introduction of a characteristic damage variable. Compos. Sci. Technol. **46**, 29–37 (1993)
13. Pakdel, H., Mohammadi, B.: Prediction of outer-ply matrix crack density at saturation in laminates under static and fatigue loading. Int. J. Solids Struct. **139**, 43–54 (2018)
14. Luterbacher, R., Trask, R.S., Bond, I.P.: Static and fatigue tensile properties of crossply laminates containing vascules for selfhealing applications. Smart Mater. Struct. **25**, 015003 (2016)
15. Gamby, D., Rebière, J.L.: A two-dimensional analysis of multiple matrix cracking in a laminated composite close to its characteristic damage state. Compos. Struct. **25**, 325–337 (1993)
16. Pakdel, H., Mohammadi, B.: Stiffness degradation of composite laminates due to matrix cracking and induced delamination during tension-tension fatigue. Eng. Fract. Mech. **216**, 106489 (2019)
17. Okabe, T., Onodera, S., Kumagai, Y., Nagumo, Y.: Continuum damage mechanics modeling of composite laminates including transverse cracks. Int. J. Damage Mech. **27**(6), 877–895 (2017)
18. Talreja, R., Varna, J.: Modeling Damage, Fatigue and Failure of Composite Materials. Woodhead Publishing Series in Composites Science and Engineering, vol. 65 (2016)
19. Ogin, S.L., Smith, P.A., Beaumont, P.W.R.: Matrix cracking and stiffness reduction during the fatigue of a (0/90)s GFRP laminate. Compos. Sci. Technol. **22**, 23–31 (1985)
20. Carraro, P.A., Quaresimin, M.A.: Stiffness degradation model for cracked multidirectional laminates with cracks in multiple layers. Int. J. Solids Struct. **58**, 34–51 (2015)
21. Tsamtaskis, D., Wevers, M., De Meester, P.: Acoustic emission from CFRP laminates during fatigue loading. J. Reinf. Plastics Compos. **17**, 1185–1201 (1998)
22. Standard test method for tension-tension fatigue of polymer matrix composite materials D3479M-96